In-Cylinder Heat Transfer Research at the U.W. Engine Research Center

G.L.Borman

Engine Research Center
& Mechanical Engineering Department
University of Wisconsin-Madison
1500 Johnson Drive
Madison, WI 53706
U.S.A.

ABSTRACT

This lecture summarizes results from engine heat transfer studies carried out by the ERC staff and students at U.W. during the past three years. The work covers instrumentation for both radiation and total heat transfer in the cylinder, boundary layer measurements and convection models to be used as subgrid models in computational fluids codes such as KIVA. Conclusions from engine tests and comparisons with models are given in abbreviated form.

INTRODUCTION

In 1987 the author collaborated with Professor Nishiwaki to review the status of engine heat transfer (1). To keep within the allotted length this lecture will not repeat any portion of that review or attempt to review publications produced since that time. Rather, this lecture will take a more parochial viewpoint and concentrate on heat transfer research carried out at the ERC since 1987. These engine heat transfer projects have concentrated on three areas; improved methods of measurement, models suitable for use in computational fluid mechanics (CFM) codes, and experimental validation of such models.

The objective is to produce models and understanding which can improve the ability to design engines and in particular to understand the relationship between heat transfer and combustion in direct injection diesel engines.

The lecture will follow through each of the three aforementioned areas, ending with some thoughts on directions for future work.

STEADY STATE FLUX MEASUREMENTS

Steady flux measurements in the cylinder are complicated by lack of accessibility and the three dimensional nature of the flow due to the geometry and the large spatial variation of the gas-side flux. The unsteady component can be calculated using a one-dimensional analysis, because the penetration of the unsteady temperature variation is typically less than 1 mm. However, the use of one-dimensional analysis can be quite inaccurate for the steady state component. One might assign a zero or cross-over point to the unsteady flux based on zero difference between the mass average gas temperature, obtained from the measured pressure, and the measured gas-side surface temperature. However, this method suffers from error due to the well known phase difference between flux and temperature difference (the "negative h syndrome"). For 3-D calculations one can use a finite difference method to calculate steady state surface flux. This requires knowing five surface temperatures and the temperature in the solid behind the center surface temperature. Figure 1 shows this configuration. Each surface couple is J-type with 1 μm vacuum-deposited chromium surface layer. This is preferable to an iron layer which can cause considerable error if made thin so as to avoid phase error. The flux thru the area $\Delta x^2/4$ with center at location 1 is

$$q_{ave} = k(T_1-T_6)/\Delta z + (2k\Delta z/\Delta x^2)(T_1-T_A) \quad (1)$$

where $T_A = (T_2+T_3+T_4+T_5)/4$

Measurements in a Cummins NH single cylinder diesel with the instrument plug replacing an exhaust valve in the head (2) showed that the correction given by the second term in Eq. 1 is small (8%) at low loads, but quite important (60%) at high loads. One might note that the instrument if used in a S.I. engine could also give data on flame travel.

TRANSIENT CYCLE EFFECTS

The heat transfer instrument described above was used by Lin and Foster (2) to investigate the effects of sudden changes in fueling level. For their experiment the engine speed and intake port

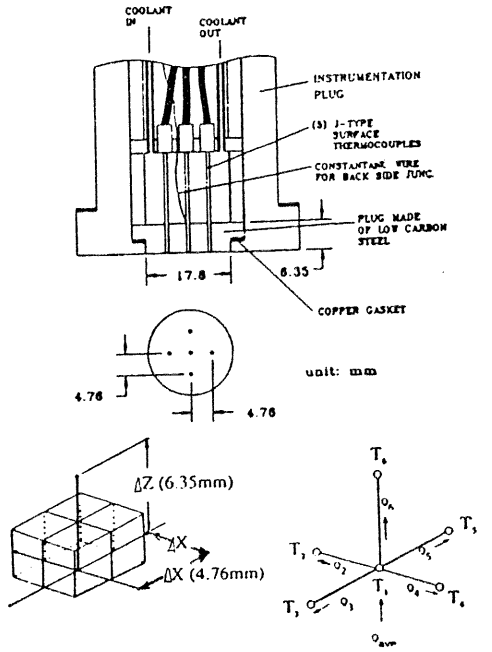

Figure 1. Schematic of flux transducer showing thermocouple locations and finite difference analysis scheme.

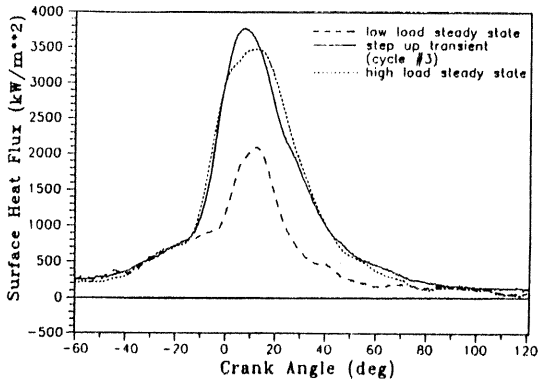

Figure 2. Comparison of surface flux at low load (ϕ = 0.3) and high load (ϕ = 0.6) steady state and the third cycle after the step-up load. (Ref. 2).

conditions were held constant. The fuel line pressure to the Cummins PT injector was then suddenly changed to either step-up the fueling level from equivalence ratio of 0.3 to 0.6 or step it down. In a typical experiment the step up portions would be periodically inserted between lower load steady state operation. The fueling level would reach its new value during the second cycle after a step-up. Figure 2 shows the effect of the cooler walls on the flux for the third cycle after a step-up. The flux has a higher peak and is slightly advanced compared to the steady state high load flux. During this third cycle the closed cycle portion of the heat transfer (from IVC to EVO) was 12.6% higher than the high load steady state value. The heat transfer change increased the ignition delay, the peak pressure, the maximum rate-of-pressure rise and the premixed fraction. However, these changes were small and the peak pressure, imep and isfc all essentially jumped to the steady state value. The heat flux and combustion effects came to the steady state within 100 cycles although it took several thousand cycles for the metal temperatures to reach steady state. It is of course understood that in a multicylinder engine the turbocharger delay effects would dominate over changes due to heat flux.

SPATIAL VARIATIONS OF FLUX

A transducer similar to the one just described was used in a CFR engine by Boggs (3). The engine was operated with premixed gaseous fuel and air both in an S.I. and an autoignition ("flameless") mode (4). In both cases it was noted that for any single cycle flux variations between surface thermocouples only 2.4 mm apart were remarkably large. A check of the diesel data (2) showed similar variations. Ensemble averages of several hundred cycles showed only the small expected spatial variations for all three combustion modes. Figure 3 shows the ensemble averaged flux for three of the couples while Figure 4 shows the flux for the same couples for a specific cycle. An experiment in which the charge was recompressed without an intervening intake process showed much reduced spatial variations. Apparently such spatial variations are characterized by the turbulence rather than by the combustion mode.

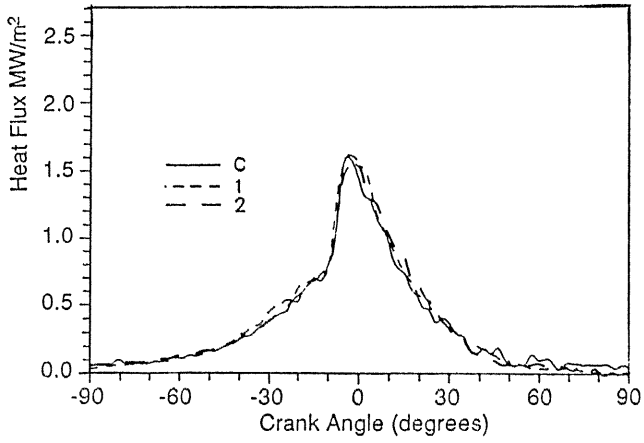

Figure 3. Ensemble averaged flux for three thermocouple surface locations each 2.4 mm apart. CFR engine, 1200 rpm, ethylene with ϕ = 0.23; intake temperature 330°C, autoignition. (Ref. 3).

Such fluctuations at the surface due to turbulence also are known for pipe flows, but typically the time scales of interest are long compared to those of the fluctuations. In engines the short combustion duration makes the fluctuations much more significant. Given these observations two questions were raised. First, is the use of 1-D analysis really valid given such instantaneous gradients in

surface temperature and second, can such variations be used to measure turbulence parameters?

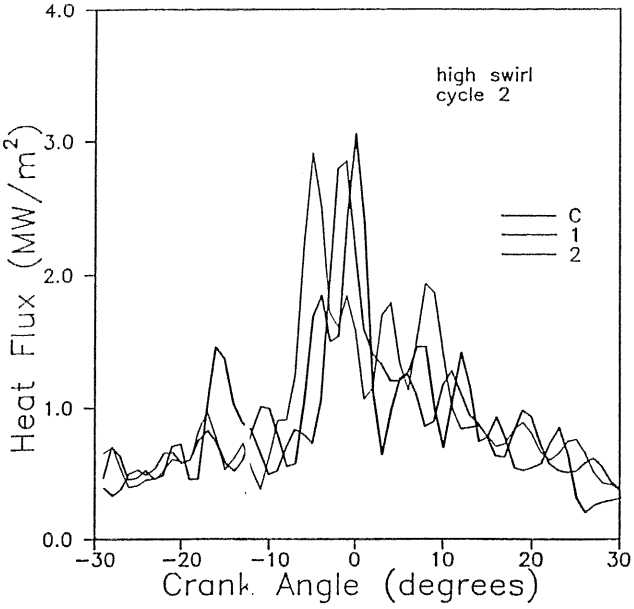

Figure 4. Flux for same locations and conditions as in Fig. 3, but for one specific cycle. (Ref. 3)

Boggs answered the first question by use of a finite element analysis which showed that the 1-D analysis error is less than 10% provided the scale of variations is greater than 1 mm. Figure 5a shows the predicted maximum error for various assumed distances between a center flux and an outer surrounding axisymmetric flux as shown in Figure 5b. In this analysis half a cosine wave was used to interpolate between the two flux values at each instant. As we shall see later, the scales are 2-3 mm.

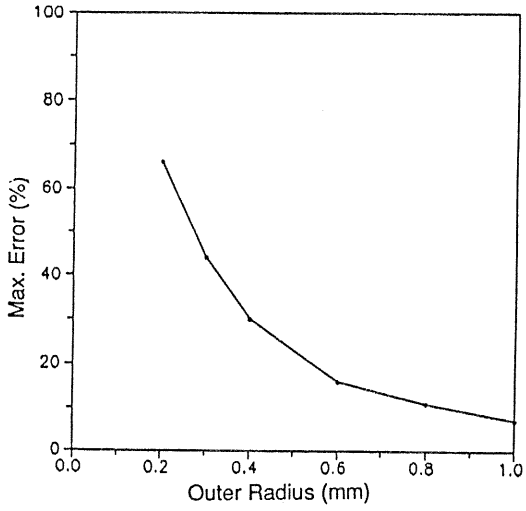

Figure 5a.

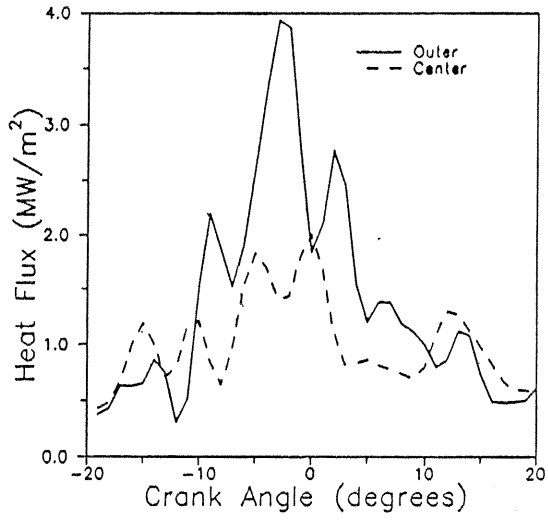

Figure 5b.

Figure 5a,b. The two flux histories shown in 5b when located with the outer flux a distance R from the center flux give the error shown in 5a if a 1-D conduction analysis is used. (Ref. 3).

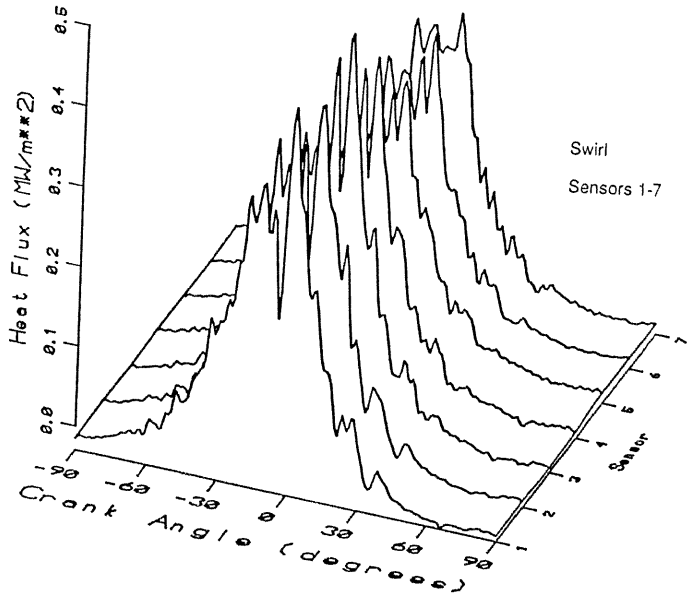

Figure 6. Flux variations during a single cycle for a motored CFR engine. The seven locations are spaced 1 mm center-to-center and each platinum film sensor is 0.8 by 0.4 mm. (Ref. 3)

In order to answer the second question a new flux sensor was required. Boggs thus constructed a sensor consisting of seven thin platinum films each 0.4 by 0.8 mm mounted in a row with 1 mm center-to-center spacing. The machinable ceramic Mecor was used as the substrate in order to improve the response. Data as still being taken for the S.I. case, thus Fig. 6 shows flux variations for motoring with swirl produced by a shrouded valve. It has been

shown that the swirl ratio for the CFR in this case is about 8 prior to tdc and then drops to about 3 at tdc.

Calculation of the turbulent flux scale is challenged by the same problems as when analyzing LDV velocity data. We may define the turbulence by use of the ensemble averaged flux $\bar{q}$ subtracted from a single record flux q_i to give the "fluctuation flux", q'_{fi}.

$$q'_{fi} = q_i - \bar{q} . \tag{2}$$

This flux is confounded by the cyclic variations of the flux. The "turbulence flux", q'_{ti}, may be defined by subtracting a "bulk flux" $\tilde{q}_i$ obtained from application of a low pass filter (300 Hz) to a single record.

$$q'_{ti} = q_i - \tilde{q}_i \tag{3}$$

In either case we may then define the flux intensity

$$q'_{rms} = \left[\sum_{i=1}^{N} q'^2_i / N \right]^{1/2} \tag{4}$$

and the heat flux correlation coefficient

$$R(x_j,x_k) = \frac{\frac{1}{N} \sum_{i=1}^{N} q'_i(x_j)\, q'_i(x_k)}{q'_{rms}(x_j)\, q'_{rms}(x_k)} \tag{5}$$

where i is the cycle number
j,k are the sensor numbers (1 to 7)

$$L \cong \sum_{k=1}^{6} [R(x_1,x_k) + R(x_1,x_{k+1})]\, (\Delta x/2) \tag{6}$$

Figure 7 shows L for motoring with a swirl flow. As expected, the fluctuation flux gave a larger scale, although both values shown are within the range anticipated from bulk velocity data. Figure 8 shows that for tumble flow the fluctuation flux gives much higher values, reflecting the much larger cycle-by-cycle variations of tumble flow compared to swirl flow.

It is interesting to note that the shape of the flux curve for the ensemble average is much more similar to that of the ensemble average theory (using ensemble average equations and a log-wall boundary layer approximation) than is that of the single cycle flux. This gives some hope that the theory (discussed later) is able to capture the ensemble average behavior even though it cannot cope with the turbulence phenomena observed during a single cycle.

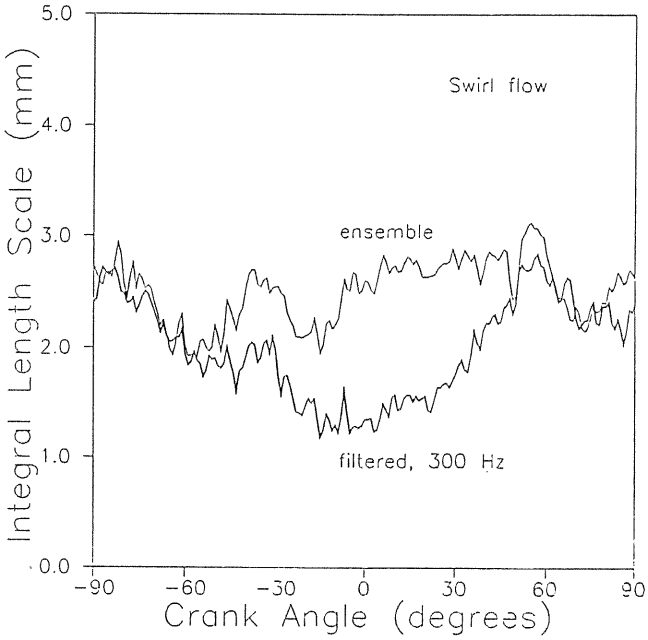

Figure 7. Length scale L as defined by Eq. 6 for motoring at 1200 rpm with shrouded valve at maximum swirl position. (Ref. 3)

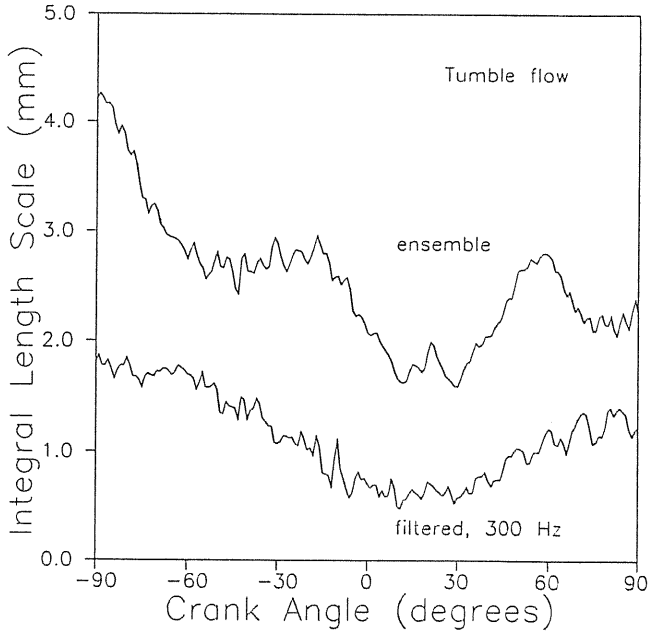

Figure 8. Length scale L as defined by Eq. 6 for motoring at 1200 rpm with unshrouded value, tumble flow. (Ref. 3).

FULL FIELD SURFACE TEMPERATURES

Because of the large variations of even the ensemble averaged flux, engine part temperature distributions are difficult to measure adequately with thermocouples or other sensors that measure at one location per sensor. Using the infra-red instrument

developed at TACOM by Dr. S. Shepard (5), piston surface temperature distributions were recently measured at the ERC using a Briggs four stroke S.I. engine modified by graduate student Wayne Moore. The modified engine has a two inch diameter window in the head which allows surface temperature measurement of a two inch diameter specimen mounted on the piston top. The window is made from zinc sulfide with a yttrium oxide surface film. Although the instrument/window did not give useful data during combustion, it gave data during gas exchange and compression and complete cycle data during engine cool-down after shut-off. The method works well for sprayed ceramic surfaces as well as metal surfaces although it is necessary to calibrate the deposit covered surface after each run or to calibrate in situ by means of a few thermocouple or Templug measurements. Because the measurements are continuous they are of particular value in thermal stress calculations and model validations.

TOTAL RADIATION FLUX

The technique of measuring radiation flux by mounting a sensor behind a window is restricted by the finite viewing angle and soot deposit on the window. Each of these problems has been solved at the ERC although a final combination of the two methods is still in progress. The problem of window soot was solved by use of a long, thin sapphire window mounted in a cavity. This design shown in Fig. 9 allowed two-color data to be taken at steady-state high load conditions without deposit calibration problems (6). The problem of field-of-view was solved by use of a Lucalox probe tip which gives the correct hemispherical signal (7). Figure 10 shows the design used for the measurements of total radiation. Figure 11 shows how the instrument was mounted in the engine. In the design shown the entire window is Lucalox and thus the window required calibration due to very thin deposit layers. To combine the two concepts one should use a Lucalox tip mounted to a very thin sapphire rod. It is not possible to use a long, thin Lucalox rod because the signal would be too highly attenuated.

Figure 12 shows the radiation flux and total flux for a point on the head just over the bowl edge of a Cummins NH engine at 1500 rpm and ϕ = 0.4, turbocharged. The line marked "14 deg" was obtained from the two color instrument shown in Fig. 9. The radiation flux calculated from the narrow 14° view data using an equivalent hemisphere correction fell only slightly short of the hemispherical measurement. However the measured time-averaged hemispherical flux ranged from 5% to 15% of total average flux over the equivalence ratio range of 0.3 to 0.5 at 1500 rpm while the corrected narrow view data gave a constant 11%. Figure 13 shows the hemispherical flux versus crankangle for three loads.

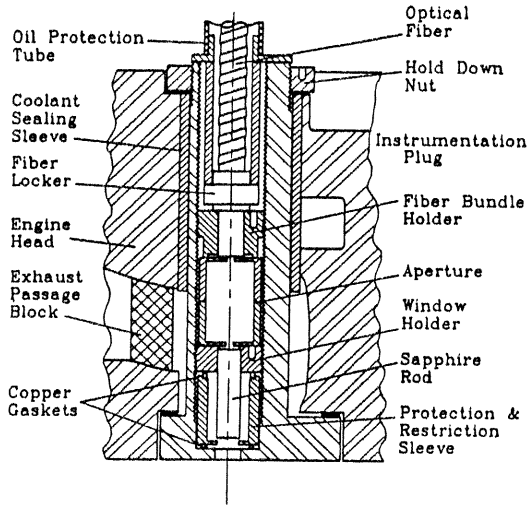

Figure 9. Schematic showing design of two-color sensor window mounted in the head of a Cummins NH engine. (Ref. 6)

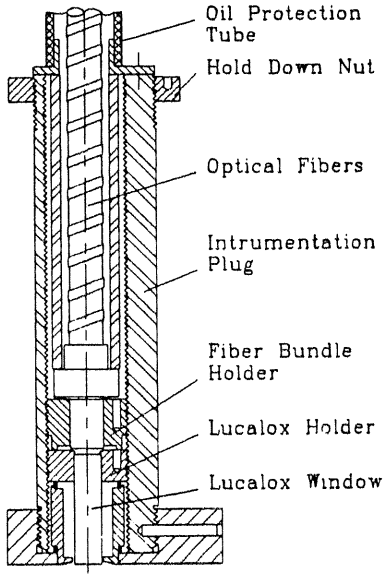

Figure 10. Schematic showing design of Lucalox sensor used to obtain hemispherical radiation in a diesel cylinder. (Ref. 7)

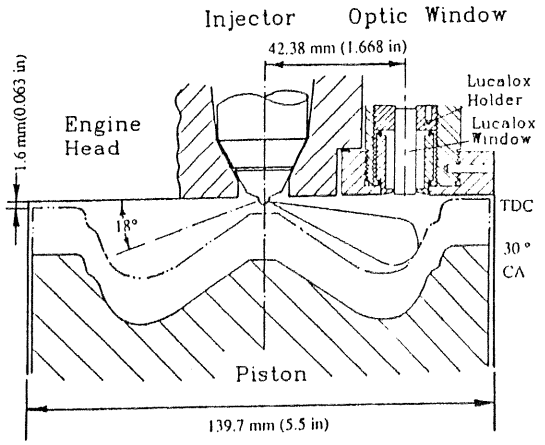

Figure 11. Schematic shows sensor of Fig. 10 mounted in engine.

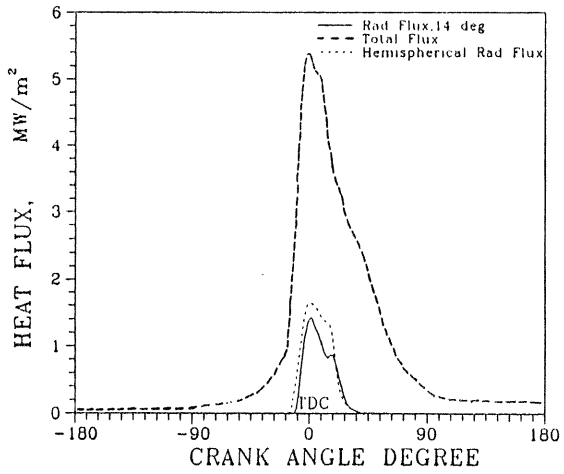

Figure 12. Total heat flux and radiation flux curves obtained by sensor of Ref. 7 and estimated from data of sensor used in Ref. 6.

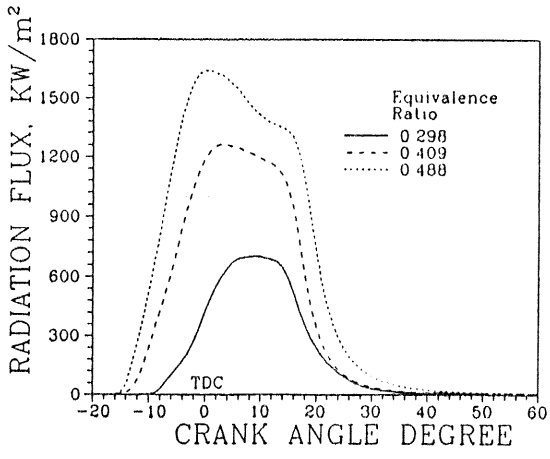

Figure 13. Radiation flux measured in Cummins NH engine with sensor as shown in Fig. 11. Engine at 1500 rpm, 201.3 KPa intake, 334 K intake, and equivalence ratio as shown. (Ref. 7)

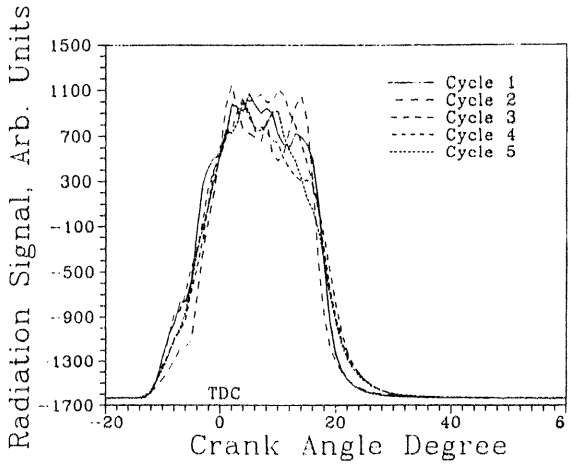

Figure 14. Variation of radiation signal for five consecutive cycles, conditions of Fig. 13, at equivalence ratio 0.409.

It is also interesting to note that cyclic variations of the peak hemispherical flux, although much reduced from those of narrow view measurements, were still ± 15% of their ensemble averaged value. Figure 14 shows the variation of the radiation signal for five consecutive cycles. The variability is much larger during the later portion (18° atdc and beyond) of the combustion period. This period is after the end of injection. One may speculate that during injection turbulent variations are less influential because the spray induced velocity overpowers them. After the end of injection the turbulence can again provide a larger influence and greater variations result.

DIRECTIONAL RADIATION FLUX

Although total radiation flux to a surface area element is necessary for both design and modeling needs it may not be sufficient for model validation. Thus a project was initiated to measure the radiation to a small portion of surface area along three different directions. Doctoral student I.S. Mohammad (8) has measured both soot temperature and concentration in three directions using a two-color method. Figure 15 shows ensemble averaged data of T and kL for the three directions shown in the insert. It should be noted that the cyclic variations are quite large for the inner regions indicating the presence of soot clouds with clear spaces between, while the outer region of the bowl has a relatively uniform concentration. The huge amount of data collected is still being analyzed at this time, but it is clear from the data that models of the sooting process using ensemble averaged equations will require very careful interpretation. It is also clear that even though this engine has low smoke levels [less than 0.3 Bosch smoke at full load] considerable air is unutilized in the central regions of the bowl.

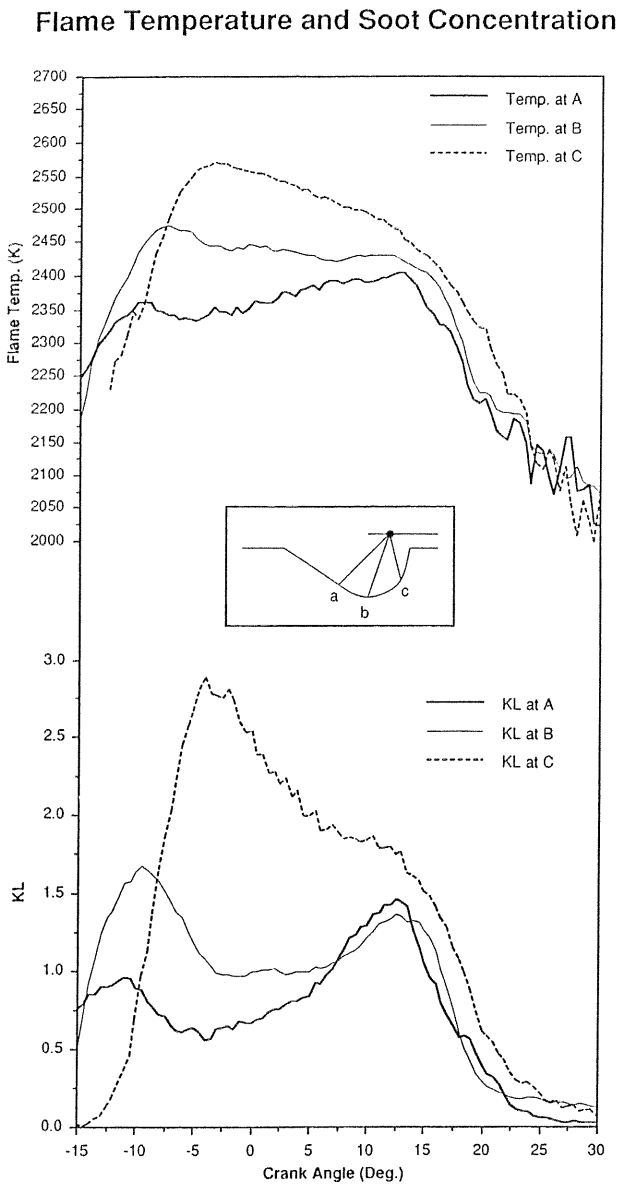

Figure 15. Ensemble averaged flame temperatures and soot concentration along three path directions using two-color method. Cummins NH engine at 1500 rpm, 273 KPa intake, 351 K intake and equivalence ratio .471.

BOUNDARY LAYER MEASUREMENTS

In addition to turbulent fluctuations that extend to the wall surface, engine boundary layer temperature profiles exhibit inflection points caused by compression and expansion. The effects of dp/dt, which appear as a source term in the energy equation (1), may also cause increases and phase changes in the peak flux. These and many other factors tend to cast doubt on the use of the log-wall function for engines. The boundary layer measurements (9) using LDV, speckle (10,11) and most recently particle image velocimetry (PIV) have been applied at the ERC to a see-through engine. The PIV data will be analyzed using an optical processor developed at the ERC by Farrell (12,13). The main use of the data thus far has been to supply parameter values to the models (9,14).

MODELS FOR THE WALL CELLS

The boundary layer is about 0.5 mm thick and thus practical considerations currently demand that CFM codes calculate the heat flux and friction by use of subgrid models. Most CFM codes thus apply the log-wall equations to the wall cells which are typically 4-6 times thicker than the boundary layer. The log-wall equations were developed from steady flow fully turbulent data for flow in pipes and over surfaces. The many differences between such conditions and an in-cylinder engine flow are listed in Table 1. The first six items apply to both motored and fired engines. The effects of unsteady flow are

Table 1 Inadequacy of Law-of-Wall Model

Engine (unknown model)	Tube (law-of-wall)
Nonsteady	Typically steady
Inflection points in temperature gradient	Temperature gradient monotonic
Core flow complicated, 3-D	Flow 2-D, simple
Compressible, dp/dt large	Incompressible
Surface temperature varies with time and position	Surface temperature constant, uniform
Turbulence may penetrate to wall	Laminar sublayer
Pressure Waves	Uniform pressure gradient
Chemical reaction	No reactions
Spray Impingement	No two-phase effects

not well known even for simpler cases, but in the engine the core flow is not only unsteady but changing from cycle-to-cycle. It has already been noted here that the heat flux shape at a given location and for a given cycle is peaked and may have several large extrema while the ensemble averaged flux is smoothed and less peaked. These affects of ensemble averaging are typical, and thus not surprising, but it is worrisome that the ensemble is not a very good representation of the individual records. The three dimensional nature of the flow is complicated by vortex shedding from protrusions such as valves, injectors and spark plugs and by the presence of many large vortex patterns generated by the intake process. Areas dominated by well directed flows, such as the squish flow dominated regions of the head near top dead center, may be better suited to the law-wall model than areas where

counter rotating, large scale vortex patterns intersect. Such stagnation like flows produce small, often intense, small vortices near the surface that can greatly enhance the heat flux (14). The log-wall may incorrectly designate such regions as having a low flux. Certainly the nature of the flow in such regions is not like flow in a tube. These boundary layer disturbances may also be enhanced by pressure waves which are superimposed on the much lower frequency compression pressure history. These waves which are generated during the rapid premixed burn in diesels and by knock in S.I. engines can have two effects. First, they may have a one dimensional effect by additional compression of the boundary layer, in effect increasing the dp/dt term in the energy equation (15). The second effect which comes from flow disturbances parallel to the surface can either decrease the heat transfer or increase it depending on the steepness of the pressure wave. We already know that steep-fronted waves caused by heavy knock in S.I. engines can increase the local flux by as much as three times (1). Of course the term dp/dt in the energy equation may also play a role even when no waves are present, such as in motoring. Its most spectacular effect, but perhaps least important, is the inflection point in the boundary layer temperature during compression and expansion, the effect previously mentioned here as the "negative h syndrome". The effect typically is only of theoretical interest because it takes place during periods of low heat transfer. (However, it may be interjected that it has a very significant effect when calculating the end of combustion from a single zone, apparent-rate-of-burning model which uses experimental pressure as an input.) For the firing case, dp/dt is highest during the period of high flux and it is difficult to sort out its effect from combustion and turbulence effects.

The last two items of Table 1 refer to the effects of combustion and sprays. For all engines, when fuel-air mixtures are in contact with the surface we have the potential for boundary layer modification by chemical reaction. For the diesel, this is primarily in the piston bowl where spray impingement also plays an important role. Models for this region must include droplet and fuel film effects on the heat transfer as well as the effects of piston surface temperature on the formation of the mixture in the bowl.

Clearly from this discussion it should be apparent that log-wall is indeed inadequate and that new approaches are needed. Several approaches have been used at the ERC in attempts to improve on the log-wall approach (16,17). The approach of Yang (16) is to solve the 1-D energy equation numerically and then obtain approximate solutions to use in KIVA. The approach of Huh (17) is to modify the log-wall to include the dp/dt source term. At present it is difficult to say if either of these approaches actually are better than the log-wall. Comparisons to even motoring data are clouded by the ability to determine the large scale flow structure at intake valve closing (IVC). One can say that details of turbulence at IVC are not important and that for low turbulence at the end of of compression and/or large dp/dt the log-wall underpredicts the flux. When data are used to obtain the friction velocity, $u^* = (\tau_w/\rho)^{1/2}$, the agreement produced by the Yang approach is good, as shown in Fig. 16. Similarly, when the local velocity dominates and can be calculated the log-wall produces good agreement with motored data (18,19,20).

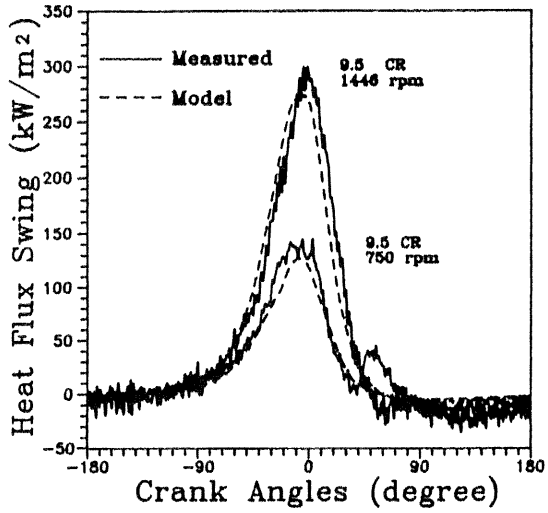

Figure 16. Comparison of measured and modeled flux for motored engine at two speeds. Model used friction velocity calculated from LDV data. (Ref. 9)

The effects of combustion can certainly produce large dp/dt values in both S.I. and C.I. engines which may in part be the cause of log-wall model underprediction of the heat transfer (17,21). Dr. Kang Huh's modified log-wall theory accounts for the term dp/dt. In this theory the temperature profile in the boundary layer is obtained by solving the one-dimensional diffusion equation

$$\frac{d}{dy}\left[(k+k_t)\frac{dT}{dy}\right] = S \qquad (7)$$

where the term S is simplified as

$$S = (C_p/R - 1)\frac{dP}{dt} + (p\,C_p/R)\,\nabla \cdot v - \dot{q} \qquad (8)$$

The terms in S are, the transient term, the work term and the chemical reaction source term. For S = 0 the result is the familiar log-wall profile, if the log-wall would indeed hold for such a case. It is important to note that in application of either the log-wall or the above modified log-wall to KIVA, two kinds of errors arise. If the boundary cell is made thinner than the boundary layer then the K-ε theory will be used to compute a portion of the boundary layer, giving an error. However as the boundary cell

is made larger, errors arise due to the temperature approximation used for the boundary cell. There must be a best single cell size which minimizes the total error, but this size has yet to be established. In Ref. (17) it is shown that a progressive decrease in grid size increased the calculated wall flux significantly, particularly the peak flux. One answer to this problem is to improve the estimate of the wall cell temperature while keeping the cell size about equal to the boundary layer thickness. Having controlled the grid size errors we may look at the effect of S, as defined in Eq. 7, on the computed flux. Table 2 shows the ratio of wall peak heat flux for $S \neq 0$. Here $\dot{q} = 0$ and the parameters dp/dt and u* were varied over their typical ranges. As already shown in Ref. 17, the importance of dp/dt depends on u*. For low turbulence and rapid combustion the effect of dp/dt is significant while for high turbulence its effect is small.

Table 2. Effects of u* and $\dot{p}$ on Calculated Heat Flux. Table values show flux divided by flux calculated from unmodified log-wall.

u*(cm/s) / dp/dt (MPa/s)	50	100	150
500	1.27	1.13	1.09
1000	1.55	1.27	1.18
5000	3.70	2.33	1.88

The term $\dot{q}$ in S arises from the effect of chemical energy release in the boundary layer. In addition to this term we also have the effect of rate of combustion in the bulk gas which dominates the heat transfer rate. An increase in turbulence or changes in swirl changes the combustion rate and this in turn changes the heat transfer. An example of this is shown in Ref. 23 where an increase in swirl caused a strong change in combustion rate shape so that the peak flux was decreased by the increase in swirl - just the opposite of the effect of swirl on motored heat transfer. Of course the high swirl heat flux was higher than the low swirl heat flux during the compression stroke up to the start of combustion.

In order to properly treat the boundary layer effects of combustion one must include the effects of turbulent mixing which tend to replace unburned fuel-air-mixture with hot products. If one recognizes that the laminar sublayer is probably nonexistant for the engine, we may suspect that energy release in the boundary layer has a small effect. Neglecting the species mixing effect we have the maximum effect, as predicted by use of Eqs. 7 and 8. Figure 17 shows a calculation for a CFR engine being run in the homogeneous auto-igniting mode. Each cell of KIVA had a chemical energy release rate controlled by a one step reaction with a simple Arrhenius rate constant. The equivalence ratio is low (0.245), but the combustion in the boundary layer had a significant

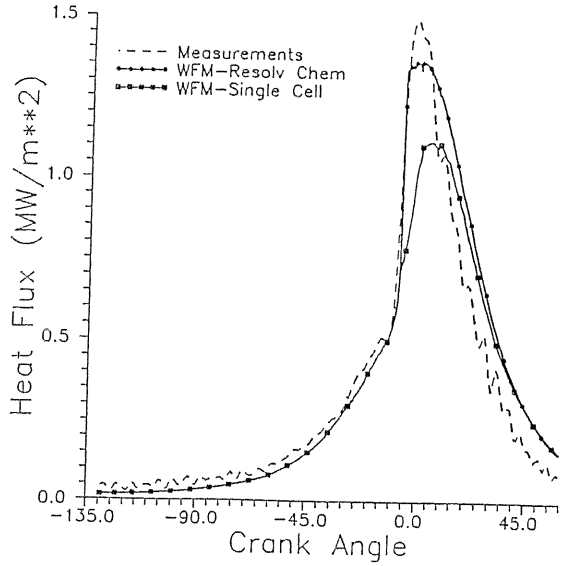

Figure 17. Comparison of model and experimental flux for a CFR engine using autoigniting combustion with ethylene fuel, equivalence ratio 0.245, 1200 rpm, inlet 315 C. (Ref. 3 and calculation by Kang Huh). Wall cell reaction by single cell and with subdivisions to resolve reaction rate. Cell size at tdc is 4 mm.

effect. This is shown by the fact that using multiple cells within the wall cell to calculate the temperature used in the rate equation greatly increased the heat flux. Note that the reaction rate constants were selected to match the calculated and experimental pressure curves. Because one cannot sort out all the sources of error here, a conclusion cannot be drawn. We may note however that calculations of Ref. 22 using a quench layer approach also show that for very thin quench layers the combustion term is important. Again, however, turbulent diffusion of species was neglected. It has been suggested that for highly elevated surface temperatures the effects of chemical reaction may actually increase the heat transfer despite the higher surface temperature (24). Reference 22 shows that this may indeed be possible. The fact that most flux data taken on the head of diesel do not show these effects is inconclusive as the head boundary layer is typically very lean. On the other hand elevation of the piston low temperature could change the combustion as well as the boundary layer heat flux. It is quite clear that piston bowl surface temperature influences the spray impingement behavior. Modeling of this behavior for diesel conditions is still underway at the ERC (25) and even if successful must still be coupled to combustion effects.

SUMMARY

Progress on predicting engine heat transfer by use of CFM codes is quite promising, but still requires considerable refinement particularly in characterizing boundary layer turbulence and the coupling

with combustion parameters. To overcome these problems CFM codes must be improved and validated for bulk flow, spray models and combustion models. It is time that a series of careful experiments be combined on the same model engine to produce such a validation. The experiments must include bulk flow measurements, detailed heat flux and boundary layer measurements and variation of combustion parameters. Such an international cooperation between Japan, Europe and the U.S.A. could greatly benefit the entire engine community.

ACKNOWLEDGEMENTS

The author wishes to thank the COMODIA 90 and MITI for making this lecture possible. The work discussed is that of the students, faculty and staff of the ERC to whom I am greatly indebted. We are very grateful for the major funding of this research which has come from the Army Research Office through support of the ERC as the Army's Center of Excellence for Advanced Propulsion Systems and through grants from the U.S. Army TACOM. Other support is also acknowledged from Briggs and Stratton Corp., Chevron Research, Cummins Engine Co., General Motors Corp., Kubota Ltd., NAVISTAR, and the U.W. Graduate School through W.A.R.F. Special thanks are also given to the many who have contributed to the Myers-Uyehara Fund.

REFERENCES

(1) G. L. Borman and K. Nishiwaki, "Internal Combustion Engine Heat Transfer," Prog. Energy Comb. Sci., Vol. 13, pp. 1-46, 1987.

(2) C.S. Lin and D.E. Foster, "An Analysis of Ignition Delay, Heat Transfer and Combustion During Dynamic Load Changes in a Diesel Engine," SAE Paper 892054, 1989.

(3) David L. Boggs, Ph.D. Thesis in Progress, Mech. Engr. Dept., U.W.-Madison.

(4) P.M. Dimpelfeld and D.E. Foster, "Predictions of Autoignition in an S.I. Engine Using Chemical Kinetics," SAE Paper 860322, 1986.

(5) S.M. Shepard and D.T. Sass, "Thermal Imaging of Repetitive Events at Above-Frame-Rate Frequencies," Optical Engineering, Vol. 29, No. 2, p. 105, Feb. 1990.

(6) J. Yan and G. Borman, "Analysis and In-Cylinder Measurement of Particulate Radiation Emissions and Temperature in a Direct Injection Diesel Engine," SAE Paper 881315, 1988.

(7) J. Yan and G. Borman, "A New Instrument for Radiation Flux Measurement in Diesel Engines," SAE Paper 891901, 1989.

(8) I.S. Mohammad, Ph.D. Thesis in Progress, Mech. Engr. Dept., U.W.-Madison.

(9) J. Yang, P. Pierce, J. Martin and D. Foster, "Heat Transfer Predictions and Experiments in a Motored Engine," SAE Paper 881314, 1988.

(10) P. Farrell and D. Verhoeven, "Heat Transfer Measurements in a Motored Engine Using Speckle Interferometry," SAE Paper 870456, 1987.

(11) S. Yamada, H. Paulsen and P. Farrell, "Heat Transfer Measurements in a Motored engine," SAE Paper 890319, 1989.

(12) P.V. Farrell and D. Goetsch, "Optical Analysis of PIV Data," Proc. Int. Conf. on Lasers and Electro-Optics, Orlando, Florida, 1989.

(13) P. Farrell and D. Goetsch, "Optical Liquid-Crystal-Television Correlator for Particle-Image-Velocimetry Processing," Optics Letters, Vol. 14, 18, 978-980, Sept. 15, 1989.

(14) H.G. Weber, "The Effect of Impinging Periodic Shock Waves on Heat Transfer for a Cooled Wall," PhD Thesis, U.W.-Madison, M.E. Dept., (1973).

(15) R.W. Goluba, "The Effect of Periodic Shock-Fronted Pressure Waves on the Instantaneous Heat Flux at the End-Wall of a Tube," PhD Thesis, U.W.-Madison, M.E. Dept, 1968.

(16) J. Yang and J. Martin, "Approximate Solution One-Dimensional Energy Equation for Transient, Compressible, Low Mach Number Turbulent Boundary Layer Flows," J. Heat Trans., Vol. 111, pp. 619-624, Aug. 1989.

(17) K. Huh, I-Ping Chang and J. Martin, "A Comparison of Boundary Layer Treatments for Heat Transfer in I.C. Engines," SAE Paper 900252, 1990.

(18) A.D. Gosman, "Computer Modeling of Flow and Heat Transfer in Engines," Progress and Prospects, COMODIA 85, Tokyo, 1985.

(19) M. Ikegami, Y, Kidoguchi and K. Nishiwaki, "A Multidimensional Prediction of Heat Transfer in Non-fired Engines," SAE Paper 860476, 1986.

(20) P. Gilaber and P Pinchon, "Measurement and Multidimensional Modeling of Gas-Wall Heat Transfer in a S.I. Engine," SAE Paper 880516, 1988.

(21) T.W. Kuo and R.D. Reitz, "Computation of Premixed-Charge Combustion in Pancake and Pent-Roof Engines," SAE Paper 890670, 1989.

(22) J. Yang and J. Martin, "Predictions of the Effects of High Temperature Walls, Combustion, and Knock on Heat Transfer in Engine-Type Flows," SAE Paper 900690, 1990.

(23) J. Van Gerpen, C. Huang and G. Borman, "The Effects of Swirl and Injection Parameters on Diesel Combustion and Heat Transfer," SAE Paper 850265, 1985.

(24) G. Woschni, W. Spindler and K. Kolesa, "Heat Insulation of Combustion Chamber Walls - A Measure to Decrease the Fuel Consumption of I.C. Engines?" SAE Paper 870339, 1987.

(25) J. Naber, Ph.D. Thesis in Progress, Mech. Engr. Dept., U.W.-Madison.